EMITTANCE SCANNER OPTIMIZATION FOR LOW-ENERGY ION BEAMS

M. P. Stockli and R. F. Welton, SNS*, Oak Ridge National Laboratory, P.O. Box 2008, Oak Ridge, TN 37831, USA

Abstract

Ion beam emittances are normally measured as two-dimensional distributions of the beam current fraction within a narrow window Δx centered at position coordinate x and a narrow window Δx′ centered at trajectory angle x′. The small fraction of the beam current found within both of these windows causes the measured emittance signals to be sensitive to noise, bias, and other unwanted signals. One example of unwanted signals is slit scattering that is discussed in detail for low-energy ion beams.

INTRODUCTION

The emittance is the key parameter to calculate the transport and losses of particle beams. It describes the six-dimensional distribution of all position coordinates along the three configuration space directions and the associate velocity coordinates. It is normally reduced into three subsets by projecting it into the two-dimensional planes {x,x′}, {y,y′}, and {z,z′}.

The experimental projection of transverse subsets, either x or y, is accomplished with a position slit placed at a number of equidistant coordinates. The slit accepts a narrow band Δx or Δy, respectively, of the beam cross section. Further downstream, a second, parallel probe samples narrow bands Δx′ or Δy′ of the corresponding trajectory angle distribution x′ or y′, respectively.

Wire harps can measure each distribution in a single shot, but the accuracy is limited by the uniformity of the amplifier gain, the wires' size, the wires' straightness, and the wires' surface condition that affects the secondary electron emission rate. The wires are likely to be uniform initially, but exposure to the beam will gradually alter some of the characteristics at rates that depend on the exposure, which varies from wire to wire. Uniformity problems can be avoided with a single slit mounted on a suppressed Faraday cup that scans the trajectory angle distribution. Highly accurate and reliable results can be expected if the beam remains stable during the time-consuming scan.

Measuring the two-dimensional distribution with adequate resolution requires a narrow slit width or thin wires. Hence most of the beam is intercepted on the entrance slit, and only a tiny fraction of the beam is measured. Due to their small amplitude, the signals are sensitive to noise, bias, and signals produced by higher order processes such as slit scattering. The effect of noise and bias can be eliminated with a self-consistent exclusion analysis as discussed in previous papers [1-3]. Data affected by higher order processes can be improved by applying model-based corrections with an accuracy limited by the model. More accurate and reliable data are normally obtained with design modifications that minimize the sensitivity to higher order processes.

Recently we have shown that data from electric sweep scanners contain signals from the beam being dumped on the electrical deflection plates. We have also shown that the amplitude of these ghost signals can be reduced by over 99% when using staircase deflection plates like the ones shown in Fig. 1 [4,5].

In this paper we discuss slit scattering and how it can be minimized for low-energy ion beams. The discussion is valid for most emittance devices scanning low-energy beams. As an example, we use the Allison scanner because it promises the most accurate emittance measurements for low-energy ion beams.

ALLISON SCANNERS

Electric sweep scanners [6] and Allison scanners [7] were introduced more than 25 years ago. Both scanners use an electric field between the two defining slits to measure the distribution of the entrance angle x′ of the beamlet passing through the first slit. Allison scanners combine the electrical sweep of the entrance-angles with a mechanical position scan that probes the position distribution x. This allows for mounting both slits on a single support base, enabling relative alignment of both slits within tight tolerances, a potential source of error. Charged particles passing through both slits are collected in a Faraday cup with suppressed secondary electron emission. A grounded light-tight shield surrounds the entire assembly to block unwanted charged particles from reaching the Faraday cup.

The voltage to angle conversion is $x' = V \cdot L_{eff}/(2 \cdot g \cdot U)$, where U is the ion's kinetic energy divided by its charge, L_{eff} is the effective length of the deflection plates, g is the

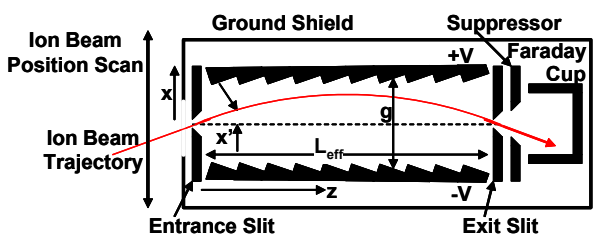

Figure 1: Schematic Allison scanner with staircase deflection plates.

*SNS is managed by UT-Battelle, LLC, under contract DE-AC05-00OR22725 for the U.S. Department of Energy. SNS is a partnership of six national laboratories: Argonne, Brookhaven, Jefferson, Lawrence Berkeley, Los Alamos, and Oak Ridge.

0-7803-8859-3/05/$20.00

average gap between the plates, and V are the voltages of opposite polarities applied to the plates. Fringing field corrections [8] improve the accuracy of the effective length over the commonly used actual length of the deflector plates [7].

The scanner can measure angles up to $x'_{max} \approx \min(V_0 \cdot L_{eff}/(2 \cdot g \cdot U), 2 \cdot g/L_{eff})$, where the first term describes the limit due to the maximum output V_0 of the voltage supplies, while the second term is the angle where the particles start to impact on a flat deflector plate.

Beam particles impacting grazingly on flat deflector plates can scatter back into the vacuum space and have a small probability of entering the Faraday cup. This process has been observed to generate signals of up to 1 % of the peak beam current entering the scanner with an angle x'_b when scanning for angles x'_s with $|x'_s - x'_b| \geq g/(2 \cdot L_{eff})$ [4,5].

The staircase deflection plates shown in Fig. 1 let the particles impact close to normal on the faces of the stairs. This drastically reduces the backscatter probability and directs the very few backscattered particles away from the Faraday cup.

Particles impacting on the flats of the stairs would aggravate the problem, and therefore the staircase angle needs to exceed all possible trajectory angles. The maximum trajectory angle at impact has been derived to be $|x'_{imax}| = (\sqrt{8}) \cdot g/L_{eff}$. This impact angle can occur when scanning at the limit of the useful geometrical range $|x'_{max}| \approx 2 \cdot g/L_{eff}$ with a beamlet entering with angle $x'_b = -x'_{max}$ [5]. Selecting a slightly larger staircase angle reduces unwanted signals to ions backscattering from the edges of the stairs, which are very narrow and rough as discussed in the next section.

LOW-ENERGY SLIT SCATTERING

Ions scattering on the slit can change their trajectory angle and/or lose some of their energy. If the predominantly inflated trajectory angles reach the Faraday cup, they cause the emittance to be overestimated.

Slit designs for high-energy beams normally use a taper to spread out the heat load of the impacting beam. Keeping the taper small minimizes the part of the slit that is too thin to completely stop the high energy beam particles.

Figure 2: Side view of Tungsten slit with a 30° taper.

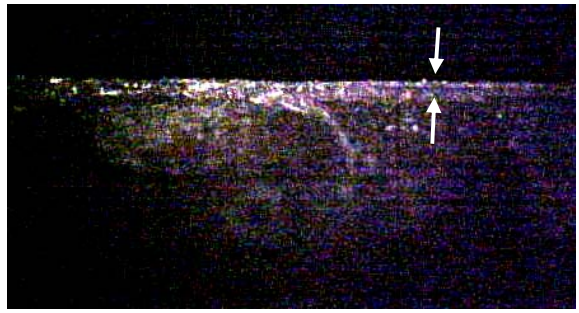

Figure 3: Slit taper at the bottom and the rough edge

Low-energy beams normally represent much smaller heat loads that may or may not require water-cooling. The smaller energy density of low-energy beams allows them them to be intercepted normal to a surface. Accordingly the flat side of the slit can face the beam and direct all backscattered particles away from the Faraday cup.

Particle impact on the side of the silts can be prevented with a downstream-facing taper that exceeds all beam trajectory angles as indicated in Fig. 1.

An optical comparator was used to determine the sharpness of different slits. Fig. 2 shows the side of a Tungsten slit with a 30° taper. The taper shown in the bottom of Fig. 3 appears to be very flat and uniform. However a ~ 25 μm wide band along the edge is quite rough with different parts of the edge having many different orientations [9].

Similar results have been obtained for Titanium slits also with a 30° taper [9] and when studying the edges of the staircase deflector plates made from stainless steel [9]. The latter two were machined twice; a rough cut was followed by a final small cut to enhance the sharpness of the edges.

The edge sharpness needs to be compared to the projected range of protons in the slit material. These have been calculated with PSTAR [10] and are shown in Fig. 4 for five different materials as a function of proton energies up to 1 MeV. It shows the range to increase with proton energy and with decreasing Z and density of the target material. In practically all cases it is much less than ~25μm width of the edges.

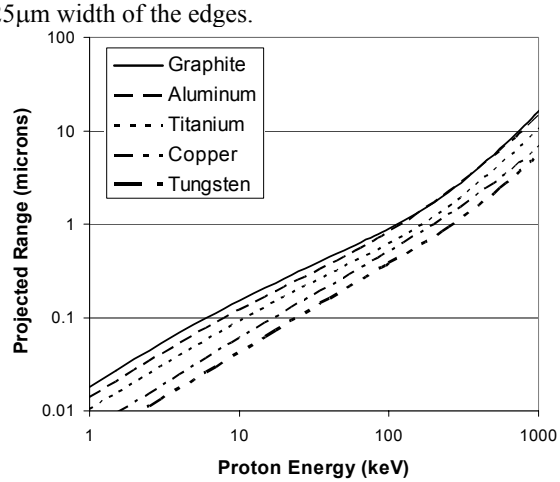

Figure 4: The projected range of protons in μm as a function of proton energy.

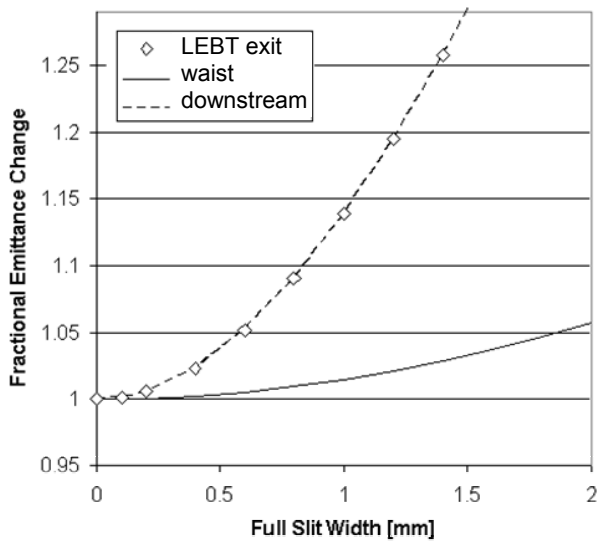

Figure 5: Fractional emittance change as function of width of the entrance and exit slit.

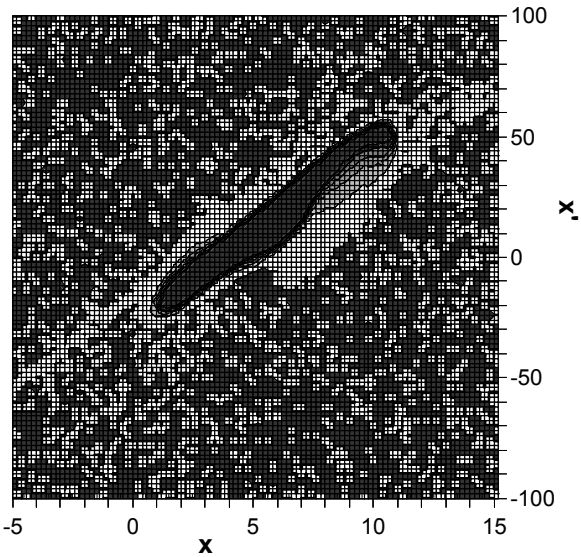

Figure 6: Emittance data obtained after the modifications described in the text.

This shows that slit scattering of low-energy particle beams is dominated by the sharpness of the slits. The roughness of the edge helps in reducing the fraction of backscattered particles that are appear to be the source of slit scattering from low-energy beams.

SLIT WIDTH OPTIMIZATION

Increasing the width of the slits allows for reducing the relative fraction of some unwanted signals such as slit scattering. Increasing the slit width decreases the resolution of the emittance measurement and therefore increases the measured emittance by an amount that depends on the area and shape of the emittance [11]. We used equations 37 and 38 from reference 11 to calculate the ratio between the apparent and the true emittance for beams being sampled by the emittance scanner used on the SNS ion source test stand [4,5]. Selecting identical widths for the entrance and exit slits, and keeping the true emittance constant, the relative error increases predominantly with the divergence of the beam. Figure 5 shows the apparent emittance increase expected when the (equal) slit widths of the entrance and exit slits are increased while measuring the unnormalized 17 π·mm·mrad beam at the exit of the SNS LEBT. The smallest errors are obtained when measuring in the waist (α=0.01; β= 0.0165 m/rad). A ten times larger sensitivity is found when measuring several cm in front (α=1.8; β= 0.07 m/rad) or behind the waist (α=–4.26; β= 0.316 m/rad). Accordingly we have increased the slit width to 0.25 mm, which causes an overestimation of $\approx$ 1 % or less. Using wider slit widths and applying corrections does not appear to be very reliable due to the strong sensitivity on α.

Figure 6 shows emittance data measured with the Allison scanner on the SNS ion source test stand after increasing the slit width to 0.25 mm and after installing the staircase deflection plates. The real current signals seen in the center are surrounded by a uniform background where noise generated a random pattern of small positive signals (white) and small negative signals (black). We are unable to identify any signature of signals from particles being scattered from the slits and/or the deflection plates.

REFERENCES

[1] M. P. Stockli, R.W. Welton, R. Keller, A.P. Letchford, R. W. Thomae, and J. W. G. Thomason, "Production and Neutralization of Negative Ions and Beams" M. P. Stockli, edt., AIP Conference Proceedings 639, Melville, New York, 2002, pp. 135.

[2] M. P. Stockli, R. F. Welton, and R. Keller, PAC'03, Portland, OR, May 2003, p. 527.

[3] M. P. Stockli, R. F. Welton, and R. Keller, Rev. Sci. Instrum. 75 (2004) 1646.

[4] M. P. Stockli et al., "Proceedings of the 16th International Workshop on ECR Ion Sources, M. Leitner, edt., AIP Conference Proceedings 749, Melville, New York, 2005, p 108.

[5] M. P. Stockli, M. Leitner, D. P. Moehs, R. Keller, and R. F. Welton, "Production and Neutralization of Negative Ions and Beams" J. Sherman and Y. Belchenko, edts., AIP Conference Proceedings 763, Melville, New York, 2005, pp. 145.

[6] J. H. Billen, Rev. Sci. Instrum. 46 (1975) 33.

[7] P. W. Allison, J. D. Sherman, and D. B. Holtkamp, IEEE Trans. Nucl. Sci. NS-30, 2204-2206 (1983).

[8] H. Wollnik and H. Ewald, Nucl. Instr. Meth 36 (1965) 93.

[9] J. Mashburn, ORNL, private communications (2005)

[10] http://physics.nist.gov/PhysRefData/Star/Text/PSTAR.html

[11] O. R. Sanders, "Accelerator Instrumentation" E. R. Beadle and V. J. Castillo, edts., AIP Conference Proceedings 212, Melville, New York, 1991, pp. 145.

